^{129}Xe nuclear magnetic resonance studies of xenon in zeolite Ca*A*

Cynthia J. Jameson
Department of Chemistry M/C-111, University of Illinois at Chicago, Chicago, Illinois 60680

A. Keith Jameson
Department of Chemistry, Loyola University, Chicago, Illinois 60626

Rex Gerald II and Angel C. de Dios
Department of Chemistry M/C-111, University of Illinois at Chicago, Chicago, Illinois 60680

(Received 5 September 1991; accepted 18 October 1991)

The average ^{129}Xe nuclear magnetic resonance (NMR) chemical shift for xenon atoms in alpha cages of zeolite Ca*A* is observed in a single peak dependent on xenon loading ($\langle n\rangle = 0.5$–8.9 Xe atoms/alpha cage) and temperature (240–360 K). The general increase of the shift with increasing average number of xenon atoms per alpha cage is shown to be due largely to the changing distribution of occupancies with increasing $\langle n\rangle$, coupled with increasing increments in the chemical shifts of Xe_n with increasing n. Except at the highest loadings, the results obtained for xenon in Ca*A* are predicted nicely on the basis of $\delta_{av}(T) = (1/\langle n\rangle)\Sigma_n n\delta_n(T)P_n(\langle n\rangle,T)$, where the fractions P_n of alpha cages containing n Xe atoms are imported from the P_n measured in xenon in zeolite Na*A*. The high loading data in Ca*A* are interpreted in terms of contributions to the average ^{129}Xe chemical shifts associated with xenon atoms in the window positions.

I. INTRODUCTION

Adsorption studies of substrates in microporous solids provide a means of characterizing the internal structure of these materials. Xenon, nonreactive and particularly sensitive to its environment, has become a widely used probe molecule. Based on the large nuclear magnetic resonance (NMR) chemical shifts of the ^{129}Xe nucleus and the previously observed large effects of intermolecular interactions in the gas phase[1–3] and in solutions,[4,5] Fraissard's pioneering work on xenon adsorbed in zeolites has made ^{129}Xe NMR spectroscopy a popular technique for characterizing zeolites, polymers, and various microporous solids.[6,7] For xenon adsorbed in a zeolite, what is generally observed in the ^{129}Xe NMR spectrum is a single peak with a resonance frequency that changes with xenon loading. Loading is usually expressed in terms of the number of atoms of xenon per g zeolite and is based on independently measured adsorption isotherms. In simple zeolites, this is usually converted to $\langle n\rangle$, an average number of Xe atoms per cavity.[8] The ^{129}Xe chemical shift inside a zeolite in the zero-loading limit is found to be characteristic of the zeolite and is roughly indicative of the size of the cavities.[6,7] The magnitude of the change of the chemical shift with $\langle n\rangle$ is also found to be characteristic of the zeolite type. Most experiments have been in the range of loadings equivalent to $\langle n\rangle = 0$–2.5 Xe atoms/cavity. Very high loading has been obtained by lowering the temperature, but this sometimes leads to problems of nonreproducible spectra when an equilibrium distribution of xenon atoms is not achieved, due to the low mobility of xenon atoms at these low temperatures.[9] There is little information on the temperature dependence of the chemical shifts of Xe in zeolites.[9,10] Changes in the ^{129}Xe chemical shifts due to the presence of other guest molecules in the cavities have raised the possibility of using Xe NMR as a means of characterizing the intrazeolitic distribution of the guest molecules.[11]

It is generally agreed that in the limit of zero loading, the ^{129}Xe chemical shift varies roughly inversely as the cavity size. There are several linear relationships that have been used to relate this ^{129}Xe chemical shift in a single xenon atom interacting with the internal surface of the zeolite to some measure of the pore diameter. The van der Waals physisorption energy $W_r(s)$ of a molecule in a zeolite cavity has been related to the ratio $s =$ molecular diameter/pore size, by Schmeits and Lucas,[12,13] by using a model which is an extension of the Onsager reaction field concept. Given the dimensions of the cavity and the sorbed molecule, the model allows a calculation of $W_r(s)$. When this ratio is 2/3, there is a large increase in the sorption energy in a spherical cavity relative to a flat surface.[14] The Xe chemical shift has been related to this curvature effect in the following empirical form:[15]

$$\delta_S = -5.35 + 33.44W_r(s), \tag{1}$$

where δ_S is the ^{129}Xe chemical shift (in ppm) extrapolated to zero coverage to eliminate shift contributions from Xe–Xe interactions. There are other similar correlations between the Xe chemical shift and cavity radius.[16–18] That the intercept apparently depends on the size of the zeolite cavity and is nearly independent of the Si/Al ratio within a range of 54 to 1.0[6,7] (the latter determines the number of counter-ions present) seems to indicate that the ions play a minimal role in determining the ^{129}Xe chemical shift.

For low loadings of xenon in zeolites, the ^{129}Xe chemical shift is generally found to increase with increasing $\langle n\rangle$ with rare exceptions. The shapes of the curves of ^{129}Xe chemical shift vs $\langle n\rangle$ depends on the type of zeolite in an unpredictable way; some are linear, others are not. Generally, they are concave upward, i.e., the increase of the ^{129}Xe chemical shift with the average number of Xe atoms per cavity becomes

 0021-9606/92/031690-08$06.00

more pronounced with higher loading. These curves serve as fingerprints of zeolite types in the sense that they are more or less reproducible in various laboratories and that they are not predictable *a priori* from zeolite structure. Although it might be suspected that these curves are largely dependent on Xe–Xe interactions, their shapes are not the same as that observed in dense xenon gas samples and they do depend on the zeolite type. What has been missing so far is a quantitative physical interpretation of these observations.

In this paper, we provide a physical interpretation to accompany new data on ^{129}Xe chemical shifts in zeolite Ca*A*, obtained for the first time as a function of loading for the entire range, up to saturation. We do this as a function of temperature as well. For our studies, we choose the *A* type zeolite in which the xenon atoms have access to identical cavities (alpha cages) which are linked directly to each other, and in which there are no other types of channels or enclosures accessible to the xenon atoms. We show that $\langle n \rangle$ obtained directly from the NMR experiments by mass balance provides an NMR determination of the adsorption isotherm as a function of temperature over a wide loading range. We provide an interpretation of the ^{129}Xe NMR data in Ca*A* in terms of the detailed information that we have obtained from the ^{129}Xe NMR spectra in Na*A*.[19] These studies in zeolite *A* provide a paradigm for the physical interpretation of the general qualitative behavior of the intrazeolitic ^{129}Xe chemical shifts.

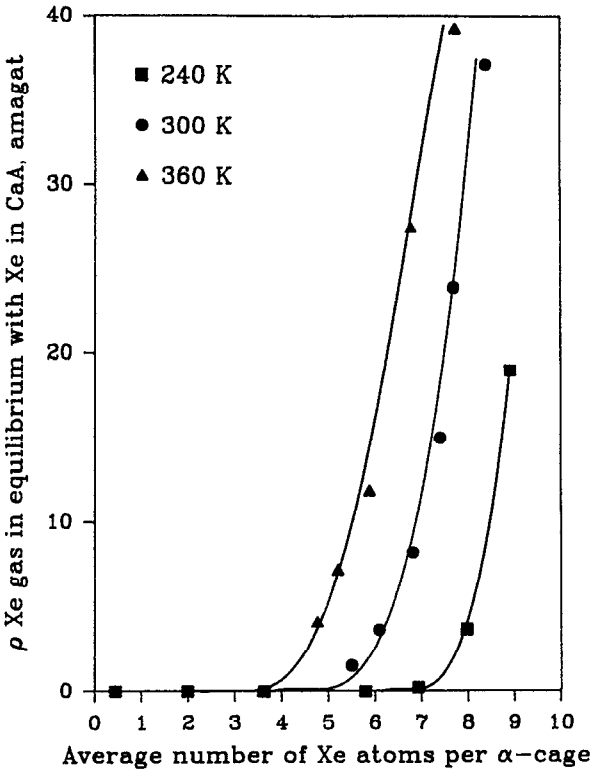

FIG. 1. The adsorption isotherm of xenon in zeolite Ca*A*, obtained from the ^{129}Xe NMR spectra. The density of the xenon gas in equilibrium with the xenon inside the zeolite is obtained from the resonance frequency of the gas peak and the average number of Xe atoms per cavity is obtained from a mass balance (1 amagat $= 2.687 \times 10^{19}$ molecules/cm^3).

II. EXPERIMENTAL RESULTS

The details of zeolite dehydration, sample preparation, and NMR spectroscopy, given in the preceding paper, will not be repeated here. The xenon in zeolite Ca*A*, unlike in Na*A*, equilibrates rapidly at 300 K or higher. We nevertheless keep the sample at the desired temperature prior to data acquisition for at least 15 min. The elaborate precautions taken with Na*A* in keeping a sample over a period of months, making sure that the sample is equilibrated, was found unnecessary for Ca*A* at room temperature.

Our work is different from others in that we use sealed samples containing an overhead pressure of xenon gas in every case. As described in the Experimental section of the preceding paper, we can determine directly from the chemical shift of the ^{129}Xe nuclei in this free xenon gas over the zeolite, the density of the xenon gas in equilibrium with the xenon inside the zeolite cages. Also, as described there, we calculate $\langle n \rangle$ the average number of Xe atoms per alpha cage directly from a mass balance of xenon in the sample. The relationship between the average number of Xe atoms per cavity and the density of the overhead gas is an adsorption isotherm, expressed here in units that are different from the usual ones. These isotherms are shown in Fig. 1 for xenon in Ca*A* at 240, 300, and 360 K. The range of measurements we are able to carry out is much greater than the range of studies reported in the literature.

In Fig. 2, we show measurements of the average ^{129}Xe chemical shift of xenon inside the zeolite Ca*A* alpha cages at 300 K, compared with the previous work of Fraissard *et al.*[8] and Dybowski *et al.*[20] The shape of the overall curve, includ-

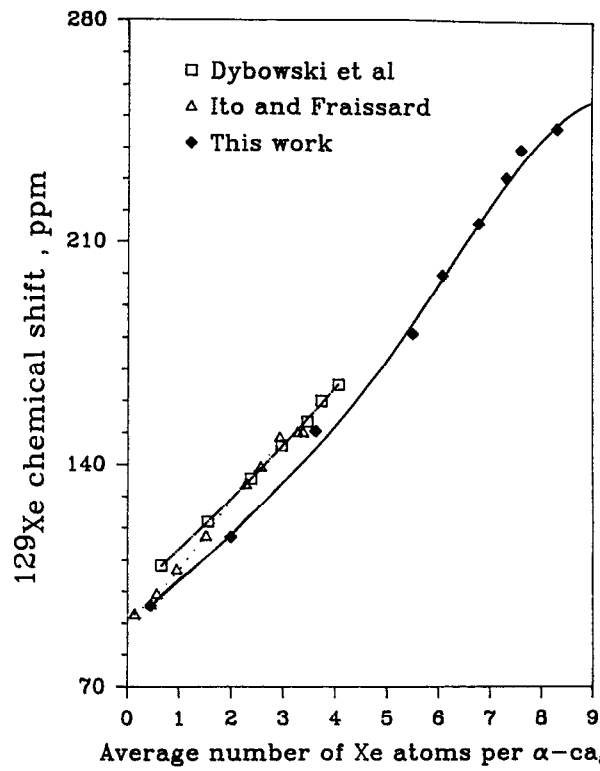

FIG. 2. The ^{129}Xe NMR chemical shift observed in samples of xenon in Ca*A*, relative to the isolated xenon atom, as a function of $\langle n \rangle$ at 300 K (this work). Data from the laboratories of Fraissard (Ref. 8) and Dybowski (Ref. 20) are also shown.

ing the downturn at near saturation, is reproducible with an independent set of samples. The only other NMR measurements of xenon in Ca*A* over all loadings that we are aware of is that of Cheung at 144 K.[21] However, at this temperature, equilibration is slow enough (the mobility of the xenon atoms is low) so that their xenon within the receiver coil may not reflect the overall $\langle n \rangle$, as indicated by the asymmetric line shapes in the early part of the experiments corresponding to $\langle n \rangle$ less than 4. Thus, their spectra may not correspond to an equilibrium situation. The lack of reproducibility that they report in other work at this temperature[9] is consistent with this. Chmelka *et al.* have shown the slow approach to equilibrium in similar systems.[11] The work presented here is the first report of ^{129}Xe chemical shifts in any zeolite for the entire range of loadings, i.e., up to maximum loading, where equilibrium is definitely achieved.

In Fig. 3 are the ^{129}Xe chemical shifts observed in the same set of samples at 240 and 360 K. The curves in Fig. 3 are by no means linear. In earlier work on xenon in various zeolites in the range $\langle n \rangle = 0$–2.5 Xe atoms/cage, many of the observed curves were nearly linear over a narrower range of measurements.[6,7] We note that the ^{129}Xe chemical shifts at the higher temperature are uniformly smaller than those at the lower temperature. Furthermore, the downturn at near saturation is also evident at 360 K, although there is no sign of it at 240 K. The intercept that would be obtained in extrapolating to zero loading is ~90 ppm at 300 K. This is essentially the same as the originally reported intercept of 90 ± 2 ppm.[8]

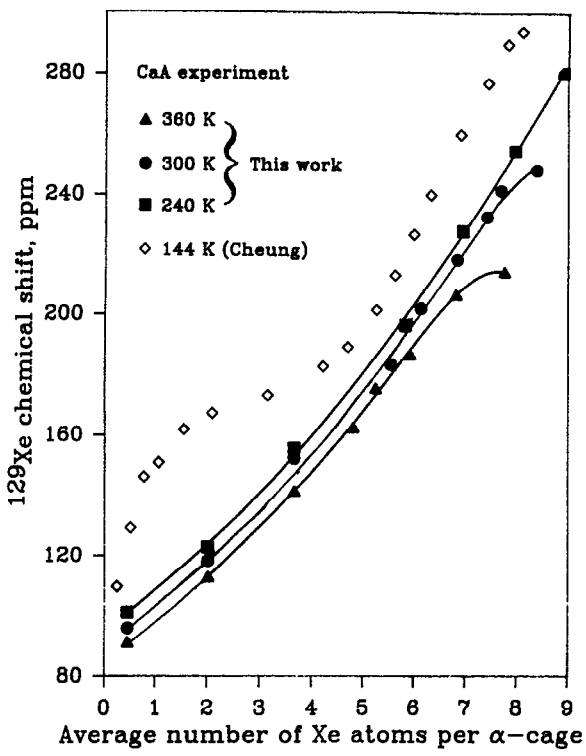

FIG. 3. The temperature dependence of the ^{129}Xe NMR chemical shift of xenon in zeolite Ca*A* (this work). Also shown are the data of Cheung at 144 K (Ref. 21).

This is the first report of a temperature-dependent study of this type. (There are, however, unpublished data for xenon in Na*Y* over a temperature range, mostly below room temperature.[22]) The intercept, the ^{129}Xe chemical shift of a single Xe atom in zeolite Ca*A*, decreases with increasing temperature from 95 ppm at 240 K to 85 ppm at 360 K. The data of Cheung at 144 K has an intercept that is consistent with this. The hump below $\langle n \rangle = 4$ in Cheung's data (also shown in Fig. 3) corresponds to spectra which are broad and asymmetric, which might indicate that $\langle n \rangle$ is not uniform over the entire sample. These results demonstrate that the intercept, which previously had been thought to be a signature characteristic of the zeolite, is dependent on temperature; temperature is a factor that has to be considered in characterization of zeolites by the ^{129}Xe NMR technique.

III. THE PREDICTION OF RESULTS IN Ca*A* FROM Na*A* DATA

In this work, we attempt to predict the observations on Ca*A* using the distributions and chemical shifts observed for the various clusters in Na*A*. There are some caveats, however, that have to be attached to these predictions. Some dissimilarities between Ca*A* and Na*A* should be noted. Besides the average chemical shifts due to interactions with Ca^{++} being somewhat different from that due to interactions with Na^{+}, there are small, but real differences between the cages in Na*A* and Ca*A* due to the differences in the number and locations of the ions. In a pseudounit cell of zeolites of type *A*, the counterions (12 Na^{+} or 6 Ca^{++} ions for Na*A* and Ca*A*, respectively) are in a relatively rigid anionic framework with formula $Al_{12}Si_{12}O_{48}^{12-}$. The exchangeable cation composition per unit cell is explicit and the framework is simple enough that the locations of these cations can be determined unambiguously.

A schematic representation of a pseudounit cell is shown in Fig. 4. An alpha cage is defined by six eight-rings (these are the windows formed by eight oxygen atoms) arranged octahedrally. Each opening is framed by four six-rings alternating with four four-rings forming a bay window. The differences between Ca*A* and Na*A* are as follows:[23] in dehydrated Ca*A* the six Ca^{++} ions lie near the centers of six of the eight six-ring sites. Approximately four-fifths of the Ca^{++} ions project out into the alpha cage and only one-fifth into the other side (the sodalite units). In dehydrated Na*A*, roughly eight Na^{+} ions lie near the centers of the eight six-rings, nearly one Na^{+} ion lies tucked away in a special site opposite a four-ring, and the remaining nearly three Na^{+} ions are accounted for by sharing each of six Na^{+} ions with another alpha cage in their locations near the centers of the six eight-ring windows. Changing the cation in going from Na*A* to Ca*A* changes the effective volume and changes the potential energy surface that describes the interaction with the Xe atoms. Although the Ca^{++} ions project out into the alpha cage, whereas the Na^{+} ions do not, there is apparently

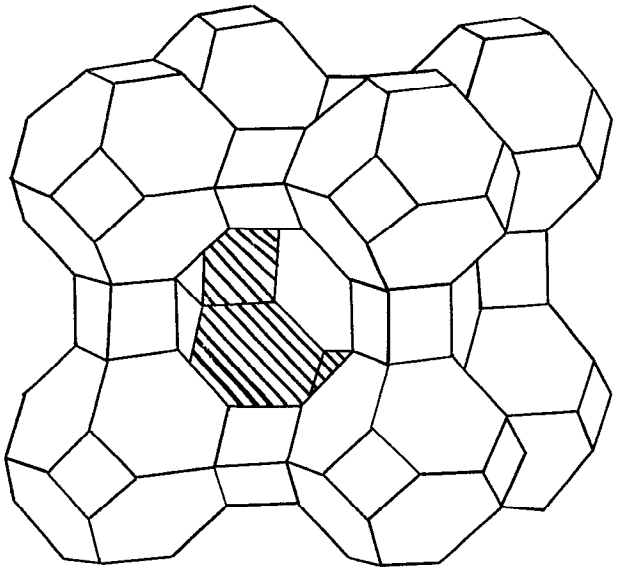

FIG. 4. A schematic diagram of a pseudounit cell of zeolite *A*. Each line represents a T–O–T unit, where T is either Si or Al. One of the eight-ring windows of an alpha cage is in the foreground, showing the "bay window" shape.

a larger available volume for xenon atoms in Ca*A* than in Na*A*, because the Ca^{++} ions are smaller than Na^{+} ions, there are fewer cations in Ca*A*, and there are no ions blocking the windows in Ca*A*. The NMR evidence does seem to indicate that for Xe atoms, there may be a bit more available volume in Ca*A* than in Na*A*. The maximum loading so far observed in Na*A* is $n = 8$. The situation is different in the Ca*A* case where average loadings slightly greater than eight have been observed in this work. Changes in the zeolite framework structure upon replacement of Na^{+} ions by Ca^{++} ions have been documented by neutron diffraction studies.[24]

It is well known from theoretical calculations that the convex internal surfaces at intersections of cavities or channels of a microporous solid correspond to high potential energy regions for an adsorbent molecule.[12,13,25,26] This is now well established by investigators using a dielectric continuum Drude model for the molecule–zeolite interaction[12,13] as well as by those who have used potentials obtained by summing up over Lennard-Jones pairwise interactions between the sorbate molecule and the oxygen atoms of the zeolite framework.[25-27] In molecular dynamics simulations, the nonpolar sorbate molecule does not frequent these locations. At all concentrations, the sorbate molecules avoid these energetically less favorable sites,[25,26] except where bulky groups on the molecule favor the intersections.[28] However, at the very high loadings in Fig. 3, some of the Xe atoms can be found in the high potential energy regions which serve as windows. Assume that the open windows in Ca*A* provide space for three more Xe atoms (i.e., a share of 0.5 Xe atom at each of six windows) in addition to the six which are easily accommodated inside the cage. The ^{129}Xe chemical shifts associated with the window locations are expected to be *lower* than those inside the alpha cage if the rough relationship postulated between intermolecular potential energy and intermolecular shielding contributions is true and if this is combined with the known less-attractive potentials associated with a molecule or atom next to *convex* surfaces (relative to flat surfaces).[12,13] The contrast between Na*A* and Ca*A* is that, while the δ_7 and δ_8 in Na*A* correspond to lower shielding (higher chemical shifts) because of the greater deshielding occurring at short range when the Xe atoms are squeezed together, the δ_7 and δ_8 in Ca*A* could correspond to somewhat higher shielding (lower chemical shift) because of the Xe atoms being found at somewhat higher potential energy locations.

We extrapolated the curve smoothly through the incremental shifts for $n = 1$–6 in Fig. 3 of the preceding paper to obtain approximate values of δ_7 and δ_8 to use in Ca*A*. These will not be correct, of course, but better than using the shifts associated with the "overcrowded" conditions in Na*A*.

By using the extrapolated chemical shifts for the Xe_7 and Xe_8 clusters and the experimental distribution of occupancies in Na*A*, we can "predict" Ca*A* spectra at the fast exchange limit. A similar prediction can be made using the same cluster shifts with the hypergeometric distribution of occupancies. We calculated the average chemical shift for ^{129}Xe at an average loading of $\langle n \rangle$ Xe atoms per alpha cage by using the hypergeometric distribution corresponding to $\langle n \rangle$ in Eq. (2)

$$\delta_{\mathrm{av}}(T) = (1/\langle n \rangle)\Sigma_n n\delta_n(T)H_n(\langle n \rangle) \qquad (2)$$

and also by using the experimentally observed distribution of Xe atoms in the alpha cages of Na*A* in Eq. (3)

$$\delta_{\mathrm{av}}(T) = (1/\langle n \rangle)\Sigma_n n\delta_n(T)P_n(\langle n \rangle, T). \qquad (3)$$

The results are compared with the experimental ^{129}Xe chemical shifts measured in Ca*A* at 300 K in Fig. 5 and at 360 K in Fig. 6.

The above discussions suggest that distributions P_n may be somewhat different for Ca*A* than those we had measured in Na*A*. The $n_{\max}$ for Ca*A* is likely somewhat larger than 8. Also, the hypergeometric distributions that we use for Ca*A* probably ought to be calculated using $n_{\max} > 8$. However, since our main point is to compare the experimental P_n with the hypergeometric distribution, we did not attempt to use two different values of $n_{\max}$. Despite all these caveats, we nevertheless use the values of P_n that we have measured in Na*A* in the prediction of xenon chemical shifts with loading in Ca*A*, and note any discrepancies with experiment as we find them.

IV. DISCUSSION

The intercept of the experimental curve for the ^{129}Xe chemical shift vs xenon loading in zeolite Ca*A* is the ^{129}Xe chemical shift for a single Xe atom in an alpha cage of Ca*A*. This is different from δ_1, the ^{129}Xe chemical shift for a single Xe atom in an alpha cage of Na*A* because of the slight differences between these cages.

The ^{129}Xe NMR spectrum observed in the progression from $(Na_{12}^{+})A$ to $(Ca_6^{++})A$ by replacing two Na^{+} ions successively with one Ca^{++} ion in the zeolite has been demonstrated by Dybowski and co-workers. The intercepts of their experimental curves follow a straight line from 97 ppm

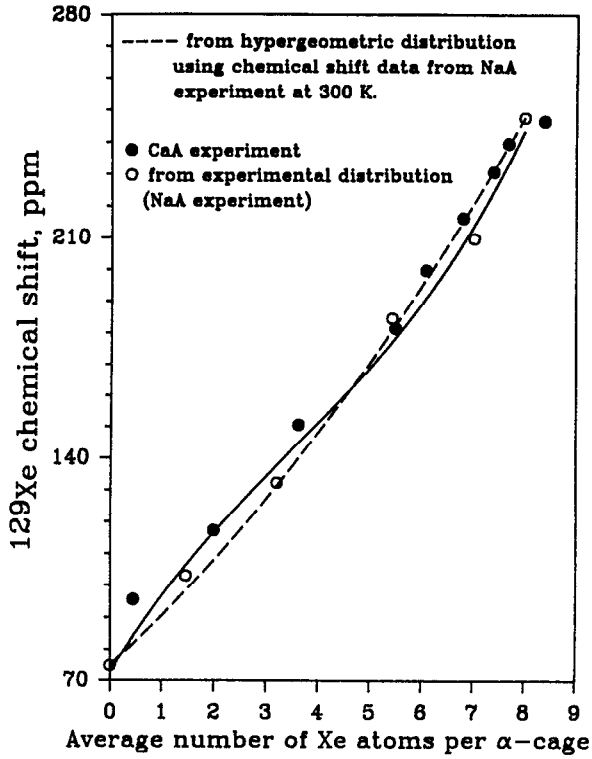

FIG. 5. Predicted ^{129}Xe NMR chemical shifts of xenon in Ca*A* based on the chemical shifts of individual Xe_n clusters at 300 K in zeolite Na*A*. The prediction based on the hypergeometric distribution [using Eq. (2) (dashed curve)] and that based on the experimentally observed distribution of xenon atoms in zeolite Na*A* at 300 K [using Eq. (3) (open circles)] are compared with the experimental data in Ca*A* itself (filled circles). The solid curve is a best fit to the open circles.

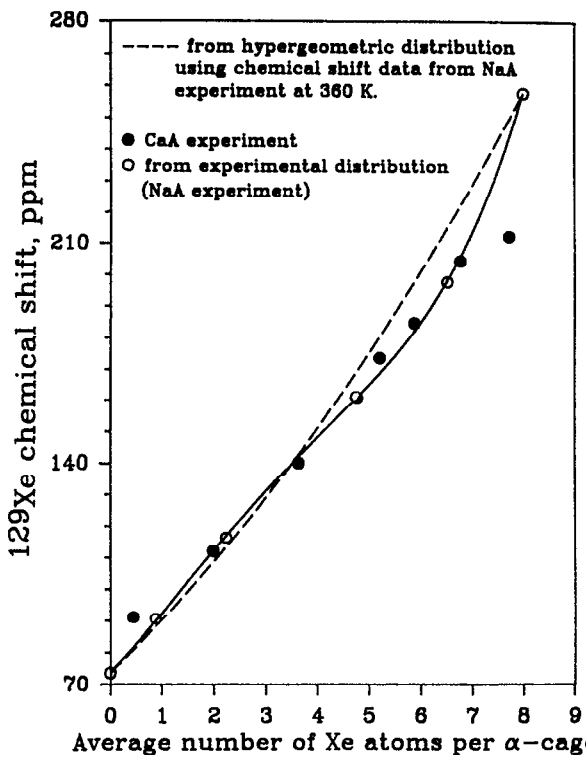

FIG. 6. The same predictions as shown in Fig. 5, except that this is for 360 K.

to our value of 75 ppm in Na*A* [19] as the number of Ca^{++} ions is changed from five to zero.[20] On the other hand, the increments $(\delta_2 - \delta_1)$, etc. are to a large extent determined by the Xe–Xe contributions to the chemical shift. Thus, while the entire predicted curve may be too low because of the different values of δ_1 for Na*A* and Ca*A*, the shape of the curve for the Xe shifts in Ca*A* vs $\langle n \rangle$ is fairly well represented by the predicted curve based on Na*A*.

There are some general points worth noting here:

(1) The general increase of the ^{129}Xe chemical shift with increasing $\langle n \rangle$ is shown to be due largely to the changing distribution of occupancies with increasing $\langle n \rangle$, coupled with slightly increasing increments in the chemical shifts of Xe_n clusters with increasing cluster size n. Even a hypergeometric distribution gives roughly the right behavior of a general increase of ^{129}Xe chemical shift with $\langle n \rangle$. We now have a better understanding of the basis for most of the curves of ^{129}Xe chemical shifts in zeolites that have been summarized in the review by Fraissard.[6,7]

(2) There is no physical basis for a straight line behavior in these curves. The straight or nearly straight lines previously obtained are symptomatic of the limited range of loadings covered by the experiments.

(3) The actual distributions of Xe atoms in the alpha cages of Ca*A* (only inferred) and in the alpha cages of Na*A* (observed in the preceding paper) are different from the strictly statistical distribution (hypergeometric) in a manner which is understandable on the basis of what is now known about potential energy functions for these systems.

(4) The shape of the predicted curve at 300 K is close to the shape of the experimental one, except at very high loadings. It might be expected that the deviations from the hypergeometric become more pronounced at lower temperatures. We note that the deviations from hypergeometric become only slightly smaller at 360 K compared to 300 K. In the limit of very high temperatures, the strictly statistical distribution would be approached.

In summary, except at the highest loadings, the results obtained for xenon in Ca*A* are nicely predicted on the basis of Eq. (3)

$$\delta_{\mathrm{av}}(T) = (1/\langle n \rangle)\Sigma_n n\delta_n(T)P_n(\langle n \rangle, T), \qquad (3)$$

leading us to believe that we have found a reasonable interpretation of the ^{129}Xe chemical shift observed in zeolite Ca*A*.

Some more specific details observed at high loading are also worth mentioning. The high loading data in Ca*A* show that the large chemical shifts δ_7 and δ_8 in Na*A* are unique to Na*A*, not observed in Ca*A*. We attribute these chemical shifts in the Xe_7 and Xe_8 clusters to the overcrowding that results from the blocking of the windows by Na^+ ions found in Na*A*. We can also suggest an explanation for the leveling off observed at both 300 and 360 K in the limit of high $\langle n \rangle$ (i.e., for $\langle n \rangle$ greater than 6 at 360 K, and for $\langle n \rangle$ greater than 7 at 300 K). This phenomenon is likely related to the δ_7 and δ_8 in Ca*A* being lower than might be expected from the incremental changes observed in δ_1 through δ_6 in Na*A* used in interpreting data in Ca*A*. A possible explanation for smaller δ_7 and δ_8 in Ca*A* may be found in the apparent connection between the ^{129}Xe chemical shift and the potential

energy, as inferred in the work of Derouane *et al.*[15] and as discussed in detail elsewhere.[29]

Schmeits and Lucas have used what is effectively a Drude model in calculating the physisorption energy of a rare gas atom physisorbed on a dielectric medium that has the form of a flat surface, a rod, a sphere, a cylindrical cavity, and a spherical cavity.[12,13] Following Buckingham's formulation (likewise based on a Drude model) for $\sigma(R)$ the nuclear magnetic shielding of a rare gas atom in the presence of another rare gas atom at a distance R,[30] we have derived relationships expressing the shielding function for a rare gas atom physisorbed on the idealized surfaces of Schmeits and Lucas. Schmeits and Lucas found that the physisorption energy is greater for a molecule inside a spherical cavity and less for a molecule on a convex surface compared to a flat surface. We have found[29] that the deshielding effect of physisorption varies with the geometry of these idealized surfaces, a larger deshielding (i.e., a larger ^{129}Xe chemical shift relative to the isolated Xe atom) for a xenon atom on the inner wall of a spherical cavity, and a smaller chemical shift for a xenon atom on a convex surface, relative to a xenon atom on a flat surface.

Various other methods have been used to estimate the potential function describing the energy of interaction between a xenon atom and the atoms of the intrazeolitic surfaces; some are based on a summation over Lennard-Jones pairwise functions between Xe and the atoms of the zeolite.[25,26] These workers find the same general qualitative dependence of the potential energy (of atom–surface interaction) on the geometry of the surface as is found in the model of Schmeits and Lucas. They find that positions next to convex surfaces such as the intersections between channels and at entrances to cavities are less energetically favorable than the minimum energy positions next to concave surfaces such a those formed by an alpha cage.[25,26] Molecular dynamics simulations show that molecules move mostly along the inner walls of the cage[27,31-35] and small nonpolar molecules such as CH_4 and Xe do not frequent the channel intersections even at 400 K.[25] In zeolite Na*Y*, molecular dynamics simulations show that the xenon atom experiences a barrier just before crossing the window and that the Xe atom remains near the inner wall of the alpha cage throughout the process of cage-to-cage migration at low concentrations.[27] Because of this nature of the potential energy surface describing the interaction of a rare gas atom with a zeolite, in the limit of very low loading, the Xe atom will tend to spend less time in the intersection between alpha cages. This means that at low loading, the chemical shifts associated with xenon atoms at locations in the intersection of two alpha cages in Ca*A* or the centers of the alpha cages do not contribute much to δ_{av}. However, at very high xenon loadings, Xe atoms are forced to spend some time at these energetically unfavorable and, we believe, lower chemical shift locations. This is our explanation of the leveling off in the Xe chemical shifts at the highest loadings in Ca*A*, as shown in Fig. 3.

A. Temperature dependence of δ_{av} in Ca*A*

The temperature dependence of the intercept in Fig. 3 appears to be small. This corresponds to a single Xe atom interacting with the internal surface of the zeolite. For a single Xe atom in zeolite Ca*A*, the average chemical shift would be given by

$$\delta_{av} = -\int d\mathbf{R}[\sigma(\mathbf{R}) - \sigma(\infty)]e^{-V(\mathbf{R})/kT}, \qquad (5)$$

where $V(\mathbf{R})$ is the potential energy of interaction between the Xe atom and the entire zeolite when the Xe atom is at position $\mathbf{R}$ and $\sigma(\mathbf{R})$ is the shielding value for the Xe nucleus when the Xe atom is at position $\mathbf{R}$ in the zeolite. $\sigma(\infty)$ is the value of the shielding of the free Xe atom. Equation (5) implies that one might expect a change toward an increasing average Xe chemical shift with decreasing temperature.

Schematic diagrams of the single Xe atom radial distribution functions in the Na*A* alpha cage at various temperatures, and a schematic diagram of the ^{129}Xe shielding, as a function of the distance from the center of the cavity are shown in Fig. 7. The shapes of the former are based on the single-particle radial distribution functions found by molecular dynamics simulations of CH_4 molecules in Na*A*.[32] The shape of the latter is based on the ^{39}Ar model for intermolecular (*ab initio*) shielding. The ^{129}Xe chemical shift of a single Xe atom in the Na*A* alpha cage at a given temperature is the average of the shielding function over all values of R weighted according to the radial distribution function. From Fig. 7, the expected temperature dependence of δ_1 in Na*A* is a decrease of chemical shift with decreasing temperature. The intercept in Fig. 3 for xenon in Ca*A* cannot be divined by using the same schematic diagrams. First, the Xe atom is not

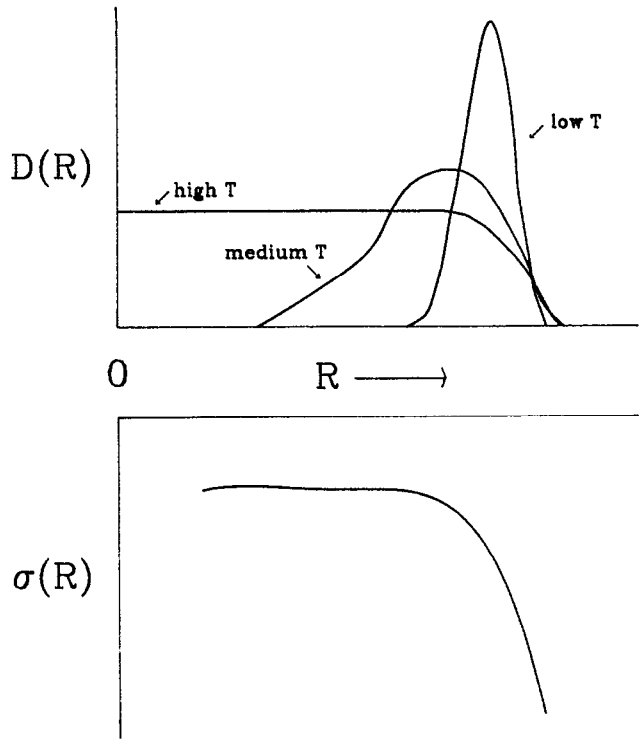

FIG. 7. Schematic diagrams of the radial distribution functions of a single Xe atom in an alpha cage of Na*A*, shown with the schematic diagram of the ^{129}Xe nuclear magnetic shielding for a Xe atom in the same alpha cage. The radial distance R is measured from the center of the alpha cage.

confined within the alpha cage, so the distribution function in zeolite Ca*A* will have a broader tail at large R from the center (the window positions), the area under this tail increasing with increasing temperature. This tail in the single-particle radial distribution function is indeed found in molecular dynamics simulations of CH_4 molecules in zeolite *ZK* 4, which has the same framework structure as zeolite *A*, but has no Al atoms and therefore no counterions in the windows or elsewhere.[33] Second, based on the Drude model for the dependence of the chemical shift on the shape of the zeolite surface, the ^{129}Xe chemical shifts predicted for the window positions in Ca*A* are smaller than for positions next to the inside wall. From all this, we expect the intercept in Ca*A* to tend toward lower chemical shifts at higher temperatures. This is indeed what we find in Ca*A* in Fig. 3. If the alpha cages of Na*A* and Ca*A* were identical, the temperature dependence of the intercept in Ca*A* should be identical to that observed for δ_1 in Na*A*. The change to lower chemical shift at higher temperatures is qualitatively the same. We do not attempt a quantitative comparison because the differences in the two alpha cages discussed above lead to differences in the temperature dependence of a single Xe atom in the alpha cages of Na*A* and Ca*A*.

For a given $\langle n \rangle$, the temperature dependence of the ^{129}Xe chemical shift in Ca*A* is contained in the temperature dependence of the δ_n of the individual clusters Xe_n and in the distribution P_n. We found, in the preceding paper, that at low loading, the actual distribution of Xe atoms in the alpha cages favors the larger clusters compared to that of the hypergeometric distribution. We based our explanation of this observation on the attractive interactions between Xe atoms, which is not accounted for in the statistical distribution of hard spheres. At lower temperatures, this tendency will be more pronounced. For low to medium loading, we find that the combination of this temperature dependence of P_n and the temperature dependence of δ_n in Na*A* agree with the direction of the observed changes with increasing temperature in the Xe chemical shift vs $\langle n \rangle$ in Ca*A*.

At much higher loadings, the observed shifts in Ca*A* are much lower than predicted in Figs. 5 and 6, leveling off rather than increasing sharply as $\langle n \rangle$ approaches 8. As already discussed above, the windows can be occupied by Xe atoms in Ca*A*, but not in Na*A*. The probability of finding Xe atoms at these less energetically favorable locations increases with increasing temperature. Thus, we observe the leveling off in Ca*A* (see Fig. 3) occurs earlier at 360 than at 300 K. The results for 240 K are consistent with a radial distribution function that has very little tail at R values corresponding to window positions even at very high loadings, when the temperature is low enough.

V. CONCLUSIONS

This combination of studies in Na*A*, in which the individual Xe clusters are observed, and in Ca*A*, in which only the fast-exchange limiting spectra are observed, provide the first comprehensive studies of ^{129}Xe NMR in zeolites over a range of temperatures and a wide range of loadings. Accompanying *ab initio* calculations in model systems provide a reasonable explanation for the observed shifts. We have presented here a physical interpretation of the observed zeolite-characterizing behavior of the single resonance peak usually observed in ^{129}Xe NMR spectra of xenon in zeolites. These studies of ^{129}Xe NMR in Na*A* and Ca*A* serve as a paradigm for the qualitative understanding of the observed ^{129}Xe shifts in many zeolites such as Na*X*, Na*Y*, *ZK* 4, *ZSM*-5, *ZSM*-11, omega, and others. We can see now why not only the intercept, but the whole shape of the curve of the ^{129}Xe NMR chemical shifts vs loading is characteristic of the zeolite. The distributions P_n of xenon atoms in the intrazeolitic cavities and the individual ^{129}Xe chemical shifts δ_n of the various clusters of Xe atoms are determined by the zeolite framework. Thus, the whole curve is characteristic of a given zeolite. There are, however, other unusual and unique behaviors of ^{129}Xe chemical shifts such as in zeolites Ca*Y* and *HZ*,[7-9] which remain to be explained.

ACKNOWLEDGMENT

This research has been supported by the National Science Foundation (Grant No. CHE-8901426).

[1] A. K. Jameson, C. J. Jameson, and H. S. Gutowsky, J. Chem. Phys. **53**, 2310 (1970).
[2] C. J. Jameson, A. K. Jameson, and S. M. Cohen, J. Chem. Phys. **59**, 4540 (1973).
[3] C. J. Jameson, Bull. Magn. Reson. **3**, 3 (1980).
[4] T. R. Stengle, N. V. Reo, and K. L. Williamson, J. Phys. Chem. **85**, 3772 (1981).
[5] T. R. Stengle, S. M. Hosseini, and K. L. Williamson, J. Solut. Chem. **15**, 777 (1986).
[6] J. Fraissard and T. Ito, Zeolites **8**, 350 (1988).
[7] J. Fraissard, Z. Phys. Chem. **152**, 159 (1987).
[8] T. Ito and J. Fraissard, J. Chem. Phys.**76**, 5225 (1982).
[9] T. T. P. Cheung, C. M. Fu, and S. Wharry, J. Phys. Chem. **92**, 5170 (1988).
[10] J. A. Ripmeester and C. I. Ratcliffe, J. Phys. Chem. **94**, 7652 (1990).
[11] B. F. Chmelka, J. G. Pearson, S. B. Liu, L. C. deMenorval, and A. Pines, J. Phys. Chem. **95**, 303 (1991).
[12] M. Schmeits and A. A. Lucas, J. Chem. Phys. **65**, 2901 (1976).
[13] M. Schmeits and A. A. Lucas, Prog. Surf. Sci. **14**, 1 (1983).
[14] E. G. Derouane, J. M. Andre, and A. A. Lucas, Chem. Phys. Lett. **137**, 336 (1987).
[15] E. G. Derouane and J. B. Nagy, Chem. Phys. Lett. **137**, 341 (1987).
[16] J. Demarquay and J. Fraissard, Chem. Phys. Lett. **136**, 314 (1987).
[17] D. W. Johnson and L. Griffiths, Zeolites **7**, 484 (1987).
[18] J. A. Ripmeester, C. I. Ratcliffe, and J. S. Tse, J. Chem. Soc., Faraday Trans. 1 **84**, 3731 (1988).
[19] C. J. Jameson, A. K. Jameson, R. Gerald II, and A. C. de Dios, J. Chem. Phys. **96**, 1676 (1992).
[20] C. Tsaio, D. R. Corbin, and C. R. Dybowski, J. Phys. Chem. **94**, 867 (1990).
[21] T. T. P. Cheung, J. Phys. Chem. **94**, 376 (1990).
[22] J. A. Ripmeester and C. I. Ratcliffe, NMR Experimental Conference, St. Louis, April 1991.
[23] J. J. Pluth and J. V. Smith, in *ACS Symposium Series*, edited by G. D. Stucky and F. G. Dwyer (American Chemical Society, Washington, D.C., 1983), Vol. 218; J. Am. Chem. Soc. **105**, 1192 (1983).
[24] J. M. Adams and D. A. Haseldon, J. Solid State Chem. **51**, 83 (1984).
[25] R. J. June, A. T. Bell, and D. N. Theodorou, J. Phys. Chem. **94**, 8232 (1990).
[26] G. B. Woods and J. S. Rowlinson, J. Chem. Soc. Faraday Trans 2, **85** 765 (1989).
[27] S. Yashonath, J. Phys. Chem. **95**, 5877 (1991).
[28] R. L. June, A. T. Bell, and D. N. Theodorou, J. Phys. Chem. **94**, 1508 (1990).
[29] C. J. Jameson and A. C. de Dios (to be published).
[30] W. T. Raynes, A. D. Buckingham, and H. J. Bernstein, J. Chem. Phys. **36**, 3481 (1962).

[31] P. Demontis, S. Yashonath, and M. L. Klein, J. Phys. Chem. **93**, 5016 (1989).
[32] E. Cohen de Lara, R. Kahn, and A. M. Goulay, J. Chem. Phys. **90**, 7482 (1990).
[33] S. Fritzche, R. Haberlandt, J. Kaerger, H. Pfeifer, and M. Wolfsberg, Chem. Phys. Lett. **171**, 109 (1990).
[34] S. Yashonath, P. Demontis, and M. L. Klein, Chem. Phys. Lett. **153**, 551 (1988).
[35] S. Yashonath, P. Demontis, and M. L. Klein, J. Phys. Chem. **95**, 5881 (1991).